

Incorporating Gradients to Rules: Towards Lightweight, Adaptive Provenance-based Intrusion Detection

Lingzhi Wang¹, Xiangmin Shen¹, Weijian Li¹, Zhenyuan Li², R. Sekar³, Han Liu¹, and Yan Chen¹

¹Northwestern University, Evanston, USA

²Zhejiang University, Hangzhou, China

³Stony Brook University, Stony Brook, USA

{lingzhiwang2025, xiangminshen2019, weijianli2021}@u.northwestern.edu

lizhenyuan@zju.edu.cn, sekar@cs.stonybrook.edu

{hanliu, ychen}@northwestern.edu

Abstract—As cyber-attacks become increasingly sophisticated and stealthy, it becomes more imperative and challenging to detect intrusion from normal behaviors. Through fine-grained causality analysis, provenance-based intrusion detection systems (PIDS) demonstrated a promising capacity to distinguish benign and malicious behaviors, attracting widespread attention from both industry and academia. Among diverse approaches, rule-based PIDS stands out due to its lightweight overhead, real-time capabilities, and explainability. However, existing rule-based systems suffer low detection accuracy, especially the high false alarms, due to the lack of fine-grained rules and environment-specific configurations.

In this paper, we propose CAPTAIN, a rule-based PIDS capable of automatically adapting to diverse environments. Specifically, we propose three adaptive parameters to adjust the detection configuration with respect to nodes, edges, and alarm generation thresholds. We build a differentiable tag propagation framework and utilize the gradient descent algorithm to optimize these adaptive parameters based on the training data. We evaluate our system based on data from DARPA Engagement and simulated environments. The evaluation results demonstrate that CAPTAIN offers better detection accuracy, less detection latency, lower runtime overhead, and more interpretable detection alarms and knowledge compared to the SOTA PIDS.

I. INTRODUCTION

Advanced Persistent Threats (APT) are becoming a growing threat to both government and industrial sectors, causing significant societal impacts [3]. The Equifax breach in 2017 resulted in the theft of vast amounts of personal data, highlighting the severe privacy and security risks [35], [42]. Moreover, attackers continuously innovate to find new ways to penetrate systems and remain undetected for extended periods. Recently, provenance-based intrusion detection systems (PIDS) have gained attention from both the security industry and academia for their causality analysis capability. However, prevailing alarm fatigue, excessive runtime overhead, and long detection latency are still open research problems in real-world scenarios [13], [38], [7], [17].

Alarm fatigue [12], [39] is a significant issue plaguing the security industry. A recent survey [1] indicates that security

analysts are required to handle an overwhelming average of 5,000 alarms daily, with a majority being false alarms. The excessive volume of alarms can lead to serious consequences. For instance, in the 2013 Target data breach [35], the malicious activities were detected and reported by security tools but overlooked by analysts, resulting in delayed response and expanded losses [11]. In practice, false alarms are equally detrimental as missed alarms. Furthermore, the time needed for threat investigation largely depends on the detection granularity and attack semantics the alarms provide, such as which system entities and events form the attack chain and how they are interconnected. The overload and ambiguity of alarms make it hard for analysts to handle these alarms effectively.

In practice, significant challenges also arise from runtime overhead and detection latency. High runtime overhead compromises the scalability of detection systems, hindering their deployment on a large scale [13]. Moreover, detection latency critically affects performance, as prolonged latency delays the response to threats, thereby impeding analysts' efficiency in managing alarms.

In academia, a recent trend of PIDS [51], [48], [9], [34] leverage embedding techniques like word2vec [34] and graph2vec [48] to encode system entities and events, and neural networks like Graph Neural Networks (GNNs) [34], [9], [51] and Recurrent Convolutional Neural Networks (RCNNs) [48] to analyze information flow and produce detection results. We refer to them as embedding-based PIDS. Although these systems have demonstrated notable achievements in detection performance, they face the following challenges:

- **High Computational Resource Cost.** Embedding-based systems need to embed the graph features into vectors, usually with deep learning techniques [48], [34], [51], [9], which require a significant amount of computational resources. Moreover, many systems require caching of embeddings and deep learning models, leading to high memory consumption [13];
- **Long Detection Latency.** Embedding-based systems take

the input structured as graphs or paths, requiring time windows [9], [25] or log batches [34], [48] in their design, which leads to the additional detection delay.

• **Uninterpretable Results.** Many systems [16], [51], [45], [34], [9], [25] only flag deviations from normal behaviors without attack semantics. Moreover, we are unable to open the “black box” of the deep learning models to better understand the detection process.

On the other hand, a group of PIDS [18], [19], [30], [46], [17] operates based on human-defined mechanisms to generate representations for system entities, propagate information flow, and trigger alarms. We refer to them as rule-based PIDS. Leveraging these rules, they take actionable leads, allowing themselves to provide semantic-rich alarms and pinpoint specific suspicious events for further investigation. Besides, the rule-based approach operates on simple arithmetic calculations, which require far fewer computational resources than complex matrix calculations by neural networks. Furthermore, some rule-based approaches can consume streaming data once it arrives, which greatly reduces storage requirements and allows fast response with minimal delay. Rule-based PIDS shows advantages in real-world detection tasks due to its fine-grained detection, semantic-rich alarms, lightweight overhead, and minimal detection delay.

Despite rule-based PIDS excelling in the aforementioned perspectives, it also faces challenges in real-world deployment. Existing rule-based PIDS suffer from the inflexibility to adapt to different environments, thus having a high volume of false alarms during detection. In SOC, analysts have to manually configure the models, which is a time-consuming process [22]. This highlights the need for an automated configuration methodology and scheme to enhance the accuracy of the rule-based PIDS. To achieve this, we require a rule-based PIDS to adjust its configuration based on the detection feedback on the training set without human interference. Thus, an automatic feedback mechanism is needed. This necessitates establishing a linkage between the configuration and the detection results, enabling the configuration to be dynamically adjusted based on the outcomes of the detection process.

In this paper, we propose CAPTAIN, a rule-based PIDS with adaptive configuration learning capability. Our work aims to leverage the advantages of traditional rule-based PIDS while enabling the system to acquire suitable configurations autonomously. Specifically, we introduce three adaptive parameters to the rule-based PIDS, giving it more flexibility during detection. We construct a learning module for these parameters. We calculate and record the gradients of each adaptive parameter, transferring the rule-based system to a differentiable function. With the help of a loss function, the gradient descent algorithm can be utilized to optimize the adaptive parameters based on the training data and thus reduce the false alarms in the testing phase.

We evaluate CAPTAIN in diverse benign and APT attack scenarios, which are drawn from the widely acknowledged public datasets [5] provided by DARPA Engagement [33] and

datasets collected from simulated environments in collaboration with a SOC. The evaluation results demonstrate that CAPTAIN can reduce false alarms by over 90% (11.49x) on average compared to traditional rule-based PIDS. Additionally, CAPTAIN achieves much better detection accuracy with less than 10% CPU usage and significantly lower memory usage and latency compared to the SOTA embedding-based PIDS. We then select a few scenarios as cases to study the explainability of the learned configurations.

All in all, this paper makes the following contributions:

- We designed CAPTAIN, a PIDS that is based on general tag-propagation rules and can adjust its rules according to normal data to reduce false alarms. This design endows CAPTAIN with the lightweight, low latency, interpretability, and fine detection granularity of rule-based PIDS while also having excellent adaptability as a learning-based PIDS.
- We parameterize the rule-based system and propose a novel differentiable tag propagation framework. In doing so, the gradient descent algorithm can be utilized to obtain the optimal parameters in different detection environments.
- We systemically evaluate CAPTAIN in various scenarios, including commonly used DARPA datasets and simulated datasets from a partner SOC. The evaluation result demonstrates that CAPTAIN can automatically adapt to various environments and provide better detection accuracy with less latency, lower overhead, and more interpretable results.

We make the code of our system, all datasets, and all experiments publicly available for future analysis and research¹.

II. BACKGROUND AND RELATED WORK

In this section, we will first introduce PIDS and highlight mainstream approaches to elucidate our design choice. Then, we introduce some background about the optimization problem, as well as describe our threat model and assumptions.

A. Provenance-based Intrusion Detection

Recently, provenance-based intrusion detection has drawn wide attention from industry and academia for its powerful correlation and causal analysis capabilities. When performing provenance analysis, the system behaviors are modeled as directed acyclic graphs, called provenance graphs [52], [26], in which nodes represent system entities, such as processes, files, sockets, pipes, memory objects, etc, and edges represent interactions between entities, such as reading files and connecting to a remote host.

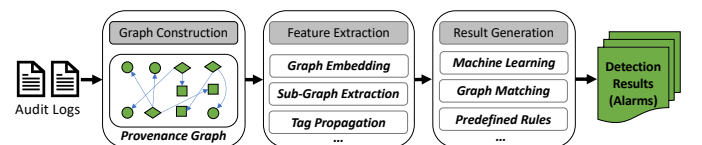


Fig. 1: A brief overview of the workflow and commonly used techniques in mainstream PIDS.

¹<https://github.com/LexusWang/CAPTAIN>

Fig. 1 illustrates an overview of typical PIDS workflow. PIDS exploits the graph nature of provenance data for whole attack information flow (data flow and control flow) analysis or multi-stage attack technique correlation analysis.

Based on the way to model and aggregate the entity information, the data/control flow, and the system behaviors, we identify two major groups of PIDS: the embedding-based approach and the rule-based approach.

Embedding-based PIDS. Embedding-based systems [25], [16], [50], [2], [51], [34], [9] use numerical vectors to represent, propagate, and aggregate the information of system entities, events, data/control flow in the graph. Various techniques in machine learning have been employed to embed the graph features into numerical vectors. Since these techniques typically require the input structured as graphs or paths, embedding-based PIDS usually adopt time windows or log batches in their design leading to the additional detection delay, which we named as *buffer time* in this paper.

Concretely, buffer time refers to the duration of the time window in which all streaming logs are stored to create a graph structure for subsequent processing. Previous studies have implemented a fixed-length window based on time [9] or the number of events [34], while some works [48] utilize the variable length window. Buffer time is crucial in real-world detection scenarios because, in the worst-case scenario, after an attack has been launched, the PIDS would have to wait for the duration of the buffer time before starting the detection procedure.

For instance, PROVDETECTOR [43] selects rare paths based on historical event frequency to generate embedding vectors for sequence learning and anomaly detection, which requires the entire path to perform detection. UNICORN[16] embeds the extracted histograms from the provenance graph and clusters the embedded graph sketches. ATLAS [2] extracts sequences from the graph and learns to classify them with Long Short-term Memory (LSTM). WATSON [50] learns the node embedding and relative event importance from the benign traces. More recent embedding-based systems employed graph neural networks [34], [9] to detect threats. While such systems can achieve better detection accuracy, they fail to provide the rationale for generated alarms. For example, SHADEWATCHER [51] provides the probability of malicious system events without further context. FLASH [34] highlights suspicious entities with causal links but does not provide further attack semantics of those interactions. In practice, more manual efforts are required to review the relevant audit logs thoroughly for further response.

Rule-based PIDS. Rule-based systems [18], [46], [30], [19], [17] leverage human-designed rules to map system entities and events to predefined semantic units (e.g., tags [18], [19], [46], TTP [30], etc.) and propagation these units along the information flow to carry out the detection results. NODOZE[17] assigns an anomaly score to each edge in the provenance graph based on the frequency it appears in the benign data and propagates the anomaly scores on the graph. POIROT [29] models APT detection as a graph pattern matching problem that aligns

manually constructed query graphs on the provenance graph. Rule-based systems have become popular due to their real-time processing capabilities and lightweight properties. However, they usually suffer low detection accuracy due to the lack of fine-grained rules and environment-specific configurations.

Table I summarizes the detection granularity and whether performing detection requires buffer time.

In this paper, we build our system using the rule-based detection method for the following reasons: 1) rule-based detection is computationally more efficient [29], [16], [18]; 2) rule-based methods are suitable for real-time detection because they can process the event stream incrementally [26]; 3) rule-based methods [18], [19], [46] offer more explainability to the detection process and results than embedding-based methods [51], [17], [44], [16], [34], [9]; 4) rule-based methods are robust against mimicry attacks [15].

TABLE I: Comparison of existing PIDS. Buffer time refers to the waiting time before threat analysis.

	Detection Granularity	Require Buffer Time
CAPTAIN	Edge	No
FLASH	Node	Yes
KAIROS	Graph ¹	Yes
NODLINK	Node	Yes
PROGRAPHER	Node	Yes
SHADEWATCHER	Edge	Yes
POIROT	Path	Yes
MORSE	Edge	No
UNICORN	Graph	Yes
HOLMES	Edge	No
PROVDETECTOR	Path	Yes
NODOZE	Path	Yes

¹Although KAIROS triggers alarms on the graph level, it can highlight anomaly nodes and edges in the subgraphs

B. Configuration as an Optimization Problem

Finding the best configuration for a rule-based PIDS can be formalized as an optimization problem, which, in short, aims to find the best elements θ in a searching space to minimize or maximize an objective function $J(\theta)$. Gradient descent is one of the most common algorithms to solve the optimization problem [37]. It utilizes the gradient of the objective function to the parameters $\nabla_{\theta}J(\theta)$ to update θ according to $\theta = \theta - l \cdot \nabla_{\theta}J(\theta)$, where l is the learning rate. Many variants have been proposed based on the gradient descent algorithm, including stochastic gradient descent [36], mini-batch gradient descent, Adagrad [14], Adam [21], and so on. We discuss more algorithms and their applicability to CAPTAIN in § VII-A.

While the optimization problem and its gradient-based solutions play a significant role in quantitative science and engineering [28], it is rarely discussed in the previous rule-based PIDS because of the following challenges. First, no existing work formally defined the adjustable parameters with clear meanings in the context of rule-based PIDS. Second, designing an objective function, calculating, updating, and saving the gradients needed in the gradient descent algorithm

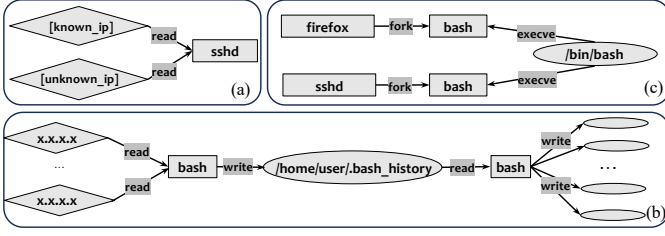


Fig. 2: Motivating examples from the Engagement dataset. (a) Communication between different IP addresses and `sshd` process. (b) Download activities via `wget`. (c) Two kinds of bash script execution we observed.

are knotty problems for a tag-based PIDS. In this paper, we introduce CAPTAIN to address these two identified gaps.

C. Threat Model & Assumptions

Similar to many previous works [19], [18], [16], [44], [17], [25], we assume that OS kernels and auditing tools are a part of the trusted computing base (TCB), which means the attackers are not able to tamper system auditing data. Meanwhile, we do not take hardware manipulation and any other attacks that leave no traces in terms of the provenance graph into consideration.

In each detection environment, we presume the availability of audit logs encompassing daily activities and devoid of any malicious activities to serve as the training data. In other words, we adopt the assumption that any alarm generated from this training data is a false alarm.

III. MOTIVATION EXAMPLES

In this section, we use three motivating examples to elucidate three common challenges encountered by rule-based PIDS, as depicted in Fig. 2.

Entity-level Distinction: Entity-level information plays a pivotal role in understanding system behaviors through provenance graphs. System entities span various categories, such as processes, files, sockets, etc. Each system entity is characterized by specific features: processes are identified by their names and command lines, files by their file paths, and sockets by their IP addresses and port numbers.

Embedding-based PIDS usually use machine learning techniques, especially from the natural language processing (NLP) field, to embed the entity-level features, such as hierarchical feature hashing [9], Word2Vec [34], and FastText [25]. However, these techniques are computationally expensive and inexplicable. On the other hand, it is hard for rule-based PIDS to distinguish the system entities for the following reasons: 1. the amount of entities is huge; 2. the detailed entity-level configuration rules vary across different environments. Therefore, in most cases, they have to apply general rules. Unfortunately, such generic configurations often result in excessive false alarms. As the motivating example in Fig. 2(a) shows, if the detection systems do not distinguish the network nodes by their IP addresses, all system entities interacting with `sshd` would inherit maliciousness from those external connections and trigger false alarms.

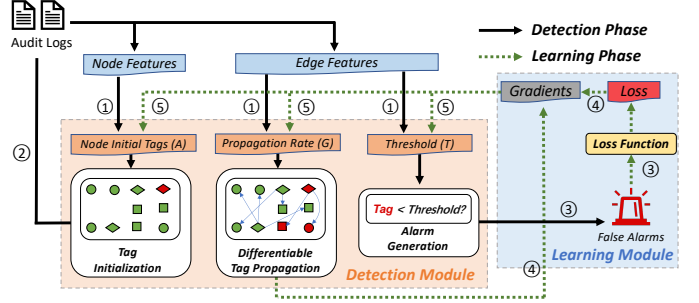


Fig. 3: The overall framework of CAPTAIN. Phases ①-⑤ show the lifecycle of the detection module and the learning module within one training epoch.

Event-level Distinction: Event-level distinction is also challenging for the rule-based PIDS during detection. System events serve as bridges that propagate the contextual information flows among system entities and form the kill chains for the attack. However, traditional rule-based PIDS find it challenging to adaptively generate fine-grained propagation and detection rules for different environments. Generic rules might lead to unsatisfying detection performance. In our motivating example in Fig. 2(c), `firefox` and `sshd` are two processes that often have network activities with various IP addresses. However, `sshd` is more likely to use `bash` to execute scripts, while it is suspicious for `firefox` to perform such tasks. Please note that in this example, the related entities and event types are the same for `firefox` and `sshd`. To distinguish such two behaviors, a very explicit rule is needed (A knotty question would be: do we need to set different rules about the “execute bash” event for each different process?). Some rule-based PIDS used frequency information in the training set to generate rules [17]. We will show later that their methods are more susceptible to the training set poisoning attack.

Dependency Explosion: Besides distinguishing system entities and events, dependency explosion is a common problem in provenance analysis [19]. In our motivating example in Fig. 2(b), we observe that the `bash` processes frequently write to and read from the `.bash_history` file. Notably, the `bash` process interacts with several potentially malicious entities as demonstrated in Fig. 2(a) and (c). Therefore, the `bash` processes tend to have relatively high maliciousness in these scenarios. Consequently, these `bash` processes propagate the maliciousness to the `.bash_history` file and then `.bash_history` spread the maliciousness among other system entities via subsequent interactions, triggering more false alarms. Many existing efforts have been made to solve this issue [32], [47], [4], [27], [24]. Unfortunately, their solutions usually require extensive instrumentation of applications/OS [4], [27], [24] and expertise, which limits the usage in the real-world system, especially in end-point host deployment. In this paper, we aim to address the dependency explosion issue via automatic learning without instrumentation on the auditing module.

IV. CAPTAIN DESIGN

A. System Overview

As shown in Fig. 3, CAPTAIN consists of two major parts: the detection module and the learning module. The detection module takes the audit logs as input and produces detection results, while the learning module leverages the false alarms produced to fine-tune the detection module during the training phase.

B. Adaptive Detection Module

As shown in Fig. 3, the detection module in CAPTAIN comprises three major components: tag initialization, tag propagation, and alarm generation. The tags contain the security states and contextual information of system entities. System entities are assigned initial tags when they appear in the system. As additional system events happen, tags propagate among system entities accordingly. At the same time, CAPTAIN determines whether to generate alarms by comparing the tags and the malicious threshold.

Tag Design: As shown in Table II, CAPTAIN uses two types of tags: data tags and code tags, which correspond to the data flow and control flow, respectively. Data tags exist on all nodes in the provenance graph, representing the maliciousness of the data. A data tag is represented as a numerical vector $\langle c, i \rangle$, where c denotes the confidentiality score of the data, and i denotes the integrity score of the data. In contrast, code tags only exist on process nodes, indicating the maliciousness of the code. A code tag holds a numerical value $\langle p \rangle$, where $\langle p \rangle$ denotes the integrity score of the code.

All scores (c , i , and p) are real numbers ranging from 0 to 1. A low confidentiality score is associated with highly sensitive data, such as passwords, while a high confidentiality score corresponds to public data. A low integrity score suggests that the data/code might be compromised and, therefore, is considered untrusted, while a high integrity score implies that the data/code is trusted.

TABLE II: Tags in CAPTAIN

Tag Type		Value Range
Data Tag	Confidentiality (c)	0 (Most Confidential) to 1 (Public)
	Integrity (i)	0 (Lowest) to 1 (Highest)
Code Tag	Integrity (p)	0 (Lowest) to 1 (Highest)

Moreover, we introduce three adaptive parameters:

- **Tag Initialization Parameter** (A) determines the initial tags of system entities.
- **Tag Propagation Rate Parameter** (G) adjusts the propagation effect of system events on tags.
- **Alarm Generation Threshold Parameter** (T) makes adjustments to the alarm generation rules.

We will elucidate how CAPTAIN uses the three parameters to achieve more flexible rule-based detection.

Tag Initialization: Proper tag initialization rules play a crucial role since they determine the initial security states of system

entities. For instance, if a socket associated with a benign IP address is assigned low integrity, it could lead to many false alarms. However, it is relatively less discussed in many previous works [19], [18]. They usually assign the initial tags based on domain knowledge without further adjustments. Although MORSE admits tag initialization policies could be learned from the previous tracing data, it did not discuss it in detail or propose a practical methodology.

We initialize the tags on the nodes when they are initially added to the provenance graph. As illustrated in Fig. 3 step ①, the detection system first checks for new system entities in the event upon receiving the system audit logs. If new entities are identified, they are added as nodes to the provenance graph and assigned initial data tags. When adding a new process node, we do not specifically initialize its code tag and data tag. A process node's code tag value is always inherited from the data tag of the libraries loaded by the process, and its data tag value is always inherited from its parents.

For non-process nodes, we define the adaptive parameter A at the node level to facilitate fine-grained tag initialization rules. Specifically, for any node $n_i \in N$ in the provenance graph, A stores its initial data tag with respect to its node feature. For example, the node features for a socket are its IP address. Then, all sockets with the same IP address will be assigned the same initial data tag.

The adaptive parameter A allows CAPTAIN to learn the fine-grained tag initialization rules at the node level. CAPTAIN's learning module refines A through the training process, which will be elaborated upon in §IV-C. The training process starts from the default value A_0 . Since we train CAPTAIN on the benign data, we set A_0 conservatively. In other words, we want to ensure all potential attacks can be captured with our initial parameter A_0 . For example, we assign all IP addresses an initial integrity of 0 so we do not miss any attackers entering through network communications.

Although the confidentiality scores could be customized in CAPTAIN, we find it hard to learn them from the false alarms on the benign training data. Instead, it often requires specific domain knowledge or personal, subjective judgments to determine what files are sensitive. Therefore, we manually set the initial confidentiality scores and do not adjust them with the learning module.

Tag Propagation: As shown in Fig. 3 step ②, once the tags are initialized, specific system events will trigger the propagation of these tags along the direction of the information flow, resulting in changes to code and data tags. We designed the propagation rules based on existing work [18], [19] as detailed in Table XI.

In CAPTAIN, tag propagation will pass and accumulate malicious intentions. Unfortunately, such a tag propagation mechanism can suffer from the dependence explosion issue [19] and lead to bad detection performance. For example, as shown in III, (`bash`, `write`, `/home/user/.bash_history`) is a common event that appears in many propagation chains of false alarms, which means this event causes large-scale maliciousness propagation

on the provenance graph. However, our investigation shows this is a commonly seen benign activity.

To mitigate such a problem, we introduce another adaptive parameter G , to regulate the propagation rate. Specifically, for any edge $e_i \in E$ identified with $(src_node_feature, event_type, dest_node_feature)$ in the provenance graph, G stores its propagation rate parameter $g_i \in [0, 1]$. Given g_i , the source node src , and the destination node $dest$, we update tag_{dest} as follows during tag propagation.

$$tag_{dest}^{new} = g_i \cdot tag_{rule} + (1 - g_i) \cdot tag_{dest} \quad (1)$$

Where tag_{rule} is the tag value given by the propagation rules defined in Table XI. Usually, it equals to tag_{src} . If g_i is close to 0, the corresponding tag propagation will lead to small changes in the tag values and vice versa. In this way, G allows CAPTAIN to fine-tune the propagation rules at the edge level.

CAPTAIN refines G through the training process in the learning module, which will be elaborated upon in §IV-C. We also conservatively establish the default values of G (G_0) to ensure all true positive alarms can be captured before the training starts. Particularly, we set $g_i = 1$ for all edge $e_i \in E$ identified with $(src_node_feature, event_type, dest_node_feature)$ to make all propagation fully effective.

Alarm Generation: The alarm generation rules determine whether the alarm should be generated and reported. As shown in Fig. 3 step ③, whenever an event happens, we will assess whether it satisfies the criteria to trigger alarms. Like tag propagation, the alarm generation depends on the alarm generation rules. As shown in Table XII, we generate alarms based on the triggering event, the subject and object tags, and the threshold. In the training set, if write events (s , $write$, o) with the same subject s and the same object o trigger many false file corruption alarms, it suggests the file corruption alarm threshold for s and o needs adjustments.

We introduce an adaptive parameter T to enable fine-grained adjustment of the alarm threshold. Specifically, for any edge $e_i \in E$ identified with $(src_node_feature, event_type, dest_node_feature)$ in the provenance graph, T stores its alarm threshold $thr_i \in [0, 1]$. For an edge e_i , the detection function is defined as follows.

$$f(e_i) = tag - thr_i = \begin{cases} malicious, & \text{if } f(e_i) < 0 \\ benign, & \text{otherwise} \end{cases} \quad (2)$$

where tag is the relevant tag on the node of interest on edge e_i . A low threshold prevents the system from generating the alarms, while a high threshold encourages the system to generate the alarms. In this way, T allows CAPTAIN to adjust the alarm threshold at the edge level.

Like A and G , CAPTAIN's learning module refines T can be refined through the training process, which will be elaborated upon in §IV-C. Before the training, we set the default thresholds (T_0) neutrally. In other words, we set $thr_i = 0.5$ for every edge e_i so that we do not encourage or suppress all alarms.

C. Configuration Learning Module

With the three adaptive parameters (A , G , and T) we defined in the previous section, the problem of adaptive configuration for the detection system is then converted to the optimization problem of the multi-variable function aiming to find the optimal values for A , G , and T . In this section, we present our efforts to solve this optimization problem with the gradient descent algorithm, including defining the objective function and constraints, calculating gradients, and searching for the optimal values.

1) *Loss Function:* The first step of solving the optimization problem is to define the objective function, i.e., the loss function in the context of learning tasks. The learning module aims to find the parameters that can reduce false alarms while maintaining the sensitivity to the true malicious events. Therefore, the loss function comprises two terms: the term of false alarms and the regularizer term.

The false alarm term mainly focuses on penalizing erroneously triggered false alarms. More specifically, an event e triggers a false alarm means $f(e)$ should be greater than 0 but it does not. Since $f(e) \in [-1, 1]$, we can use the Mean Squared Error $(y_e - f(e))^2$ as the loss function for all events that trigger a false alarm. y_e is set as 1 for those benign events, and -1 for the malicious events. Because we only use benign data for training, all y_e should be 1. Please also note that we do not calculate the loss for the correctly classified events, i.e., we do not make $f(e)$ close to 1 if $f(e)$ is already greater than 0. This is because the events that do not cause alarms are significantly more than the alarm-triggering events, considering them, therefore, is inefficient and would make the detection system insensible to the malicious events. Thus, the false alarm term in the loss function can be formalized as

$$\mathcal{L}(e) = \max(0, (1 - f(e))^2 - 1) \quad (3)$$

Next, we introduce the second component: the regularizer term. As we mentioned, CAPTAIN is trained on benign data to learn the normal behaviors in the detection environment. This is due to the fact that benign behaviors on a system are more consistent than attack activities. Another reason is the malicious training data is much harder to acquire. However, a big challenge is how to guarantee that the detection capability would not be affected if there is no malicious sample in the dataset, i.e. we would not be too lenient to capture the true alarm when reducing false alarms.

To capture the potential malicious events as much as possible, the adaptive parameters are configured conservatively. During training, we only want to make small adjustments to a small portion of the parameters according to the benign data to reduce the false alarms. For the rest parameters, we would like to keep them as conservative as possible so that the sensitivity to the maliciousness is not compromised.

In the area of machine learning, One-class classification (OCC) algorithms are proposed to deal with the situation where only one class of samples is available in the training set [20]. Inspired by [40], [41], we add a regularizer term in

the loss function to avoid the parameters becoming too lenient when the malicious training sample is absent. The essential thought is to make the adaptive parameters as close to the default values (A_0, G_0, T_0) as possible. By minimizing the l_2 distance between the adaptive parameters and the default values, we protect the detection capability during training. Therefore, the detection loss can be formalized as

$$Loss = \sum_{e \in E} \mathcal{L}(e) + \alpha \|A - A_0\|_2 + \gamma \|G - G_0\|_2 + \tau \|T - T_0\|_2 \quad (4)$$

where, α , γ , and τ are the regularizer coefficients.

2) *Differentiable Detection Framework*: One of the fundamental steps of using gradient descent algorithms is calculating the gradient of each variable. To adjust the adaptive parameters based on the loss function, we need to implement a differentiable rule-based PIDS, which allows us to keep the gradients of the adaptive parameters with respect to the *Loss*.

According to the chain rule, for the parameter a_n , we have

$$\frac{\partial Loss}{\partial a_n} = \frac{\partial \mathcal{L}}{\partial f} \cdot \frac{\partial f}{\partial a_n} + \alpha \quad (5)$$

The equations for g_e and thr_e hold similarly to Eq. 5.

As mentioned before, the most challenging part of building an adaptative rule-based PIDS is to compute the gradients, i.e., $\partial f / \partial a_n$, $\partial f / \partial g_e$, and $\partial f / \partial thr_e$. This is because the rule-based detection process is usually modeled as the branch selection based on rules, rather than a differentiable function. To the best of our knowledge, no previous work has formalized or recorded the gradients of parameters in a tag-based PIDS. In CAPTAIN, we model the detection process as a differentiable function and calculate the gradients of each adaptive parameter defined in § IV-B. When the tags are propagated, the corresponding gradients are updated and recorded. In so doing, we associate the adaptive parameters with the loss, making it possible to perform the gradient descent algorithm to find the optimal parameters that minimize the loss.

As per Eq. 2, $\partial f / \partial thr_e = -1$. This means every time when we want to increase the value of f (the direction of benign), we have to decrease the value of thr_e , and vice versa. This aligns with our intuition because in our framework, a lower tag value means more maliciousness. Therefore, if we want to be more lenient in the detection, we should set a lower threshold.

The formalization and calculation of $\partial f / \partial a_n$ and $\partial f / \partial g_e$ are more complicated. According to Eq. 2, calculating the gradients of f is essentially computing the gradients with respect to the variable tag for each node.

We start from the gradients of a_n . According to the propagation policies in table, tag_{rule} is either $\min(tag_{src}, tag_{dest})$ or a constant c . If $tag_{rule} = c$, then

$$\frac{\partial tag_{dest}^{new}}{\partial a_n} = (1 - g_e) \frac{\partial tag_{dest}}{\partial a_n} \quad (6)$$

If $tag_{rule} = tag_{src}$, then

$$\frac{\partial tag_{dest}^{new}}{\partial a_n} = g_e \frac{\partial tag_{src}}{\partial a_n} + (1 - g_e) \frac{\partial tag_{dest}}{\partial a_n} \quad (7)$$

Please note that if $tag_{rule} = tag_{dest}$, i.e. we do not need to update the tags of the *dest* node, the gradients of *dest* are unchanged as well.

Since a_n is defined as the initial value of the tag on node n , the initial gradient of a_n is

$$\frac{\partial tag_{n'}}{\partial a_n} = \begin{cases} 1, & \text{if } n' = n \\ 0, & \text{if } n' \neq n \end{cases} \quad (8)$$

Then we focus on the gradient of g_e , which is more complex because it exists in the equation explicitly. Therefore, the equations of calculating the gradients are slightly different. Here we use M to represent $\min(tag_{src}, tag_{dest})$ for the succinctness.

$$\frac{\partial tag_{dest}^{new}}{\partial g_{e'}} = \begin{cases} g_e \frac{\partial M}{\partial g_{e'}} + (1 - g_e) \frac{\partial tag_{dest}}{\partial g_{e'}}, & e \neq e' \\ g_e \frac{\partial M}{\partial g_e} + (1 - g_e) \frac{\partial tag_{dest}}{\partial g_e} + M - tag_{dest}, & e = e' \end{cases} \quad (9)$$

As previously stated, g_e are set according to the event features (*src_node_feature, event_type, dest_node_feature*). Therefore, before the propagation happens,

$$\frac{\partial tag_n}{\partial g_e} = 0, \forall e \in E, \forall n \in N \quad (10)$$

We use Eq. 10 to initialize the gradient of g_e and update them according to Eq. 9. Besides, similar to the case of a_n , when the tag is not updated, i.e. $M = tag_{dest}$, we do not have to update the gradients on the related nodes.

In summary, to employ the gradient descent algorithm, we calculate the gradients of the adaptive parameters with respect to the loss. We first calculate the initial gradient for each node. Afterward, the gradients are updated according to our equations when the tags are propagated.

3) *Training and Testing*: In the previous section, we create a differentiable tag propagation framework to calculate the gradients of the adaptive parameters with respect to the loss. We can now utilize the gradient descent algorithm to optimize the adaptive parameters. In machine learning, this process is commonly referred to as “training”. The learned parameters are stored as a customized configuration, which is then used to set up our system prior to testing.

As shown in Fig. 3, an epoch in training comprises the forward and backward propagation. Before we start learning, we configure all adaptive parameters, A , G , and T , as the default settings A_0 , G_0 , and T_0 . Instead of random initialization[8], we want to use the most conservative setting as the starting point to keep the sensitivity to the maliciousness during training.

When CAPTAIN processes the events, tags are propagated among the graph, updating the gradients according to Eq. 7 and Eq. 9, and generate the detection results. Next, we calculate the loss according to the detection results and back-propagate the gradients of loss according to Eq. 5. Finally, we update the parameters in the opposite direction of the gradient as follows:

$$p_{new} = p_{old} - l \cdot \frac{\partial Loss}{\partial p_{old}} \quad (11)$$

where p is the adjustable parameters (which could be a_n , g_e , or thr_e), p_{new} is the new parameters, p_{old} is the old one,

$\frac{\partial Loss}{\partial p_{old}}$ is the gradient, and l is the learning rate. We repeat the training process when the maximum epoch is reached or the changes in the result become sufficiently small.

Before testing, we configure the parameters according to what we learned in the training stage. Then, CAPTAIN can process audit data and conduct detection as introduced in § IV-A.

V. IMPLEMENTATION

The entire system (including data parsing, tag initializing, tag propagating, alarm generating, and training/testing framework) consists of 5KLoC of Python. We will release the code of our system to the public to facilitate further reuse, research, and improvements².

We implement the differentiable tag-propagation framework by creating two dictionaries for each tag to store the gradients with respect to A and G . As for T , because its gradients are unrelated to the node tags, there is no need to store them within the node. The space used to store those gradient dictionaries during training is analyzed in § VI-C2 and § C-B

VI. EVALUATION

Our evaluation aims to answer the following five research questions: 1) How effectively can CAPTAIN detect the attacks, especially in terms of reducing false alarms? 2) How efficient is CAPTAIN compared with the SOTA PIDS in terms of detection latency and runtime overhead? (§VI-C) 3) How robust is CAPTAIN against adversarial attacks such as mimicry attacks and data poisoning attacks? (§VI-D) 4) How do different components affect the training outcome and the detection performance of CAPTAIN? (§VI-E) 5) Can CAPTAIN acquire explainable knowledge via our learning module? (§VI-F)

A. Experiment Settings

1) *Datasets*: We evaluate CAPTAIN using public forensic datasets from the DARPA Transparent Computing program and datasets generated within simulated environments in collaboration with a professional SOC. Table VIII provides an overview of all datasets.

DARPA Datasets. The DARPA Transparent Computing program was organized between 2016 and 2019 to perform several red team assessments. In two weeks, the data collecting teams deploy data collectors on several target hosts [33], which are the target of red teams. We use the public-available datasets from Engagement 3 (E3) and Engagement 5 (E5) in our evaluation. §A-A provides a detailed description of attacks performed in relevant DARPA datasets.

Simulated Environments. Moreover, we collaborate with an industry SOC to acquire additional datasets within realistically simulated scenarios to avoid the problem of “close-world data” [25]. Specifically, the security company furnishes detailed host setups from real-world operating environments, including system configurations and enumerations of active applications. Subsequently, we simulate APT attacks [10] employing the Atomic Red Team framework [6] and leveraging

malware sourced from online repositories [23]. The simulated scenarios encompass five APT attacks across three distinct real-world operational settings, elaborated in detail in §A-B.

Data Labeling. For each attack scenario, we label entities and events on the kill chains as malicious and others as benign, according to the provided attack report. Although previous work [45], [34] provided entity-level data labels in their open-sourced repository, they did not specify the data labeling strategy or context. We also observed that the amount of malicious labels in their dataset is excessively large (e.g., over 12 thousand system entities were marked as malicious within a 30-hour period on the CADETS from Engagement 3), which is impractical for a real-world SOC. Thus, we decided to use our data labels in the following evaluation for a fair and unbiased comparison between CAPTAIN and the baseline systems.

Note the attack report is written in natural human language, making it challenging to map it to the records in raw auditing logs. Therefore, we make our data labels publicly available to facilitate future research.

2) *Experiment Setup*: We deployed CAPTAIN and performed all experiments on an Ubuntu 22.04.3 Linux Server with an Intel(R) Xeon(R) Platinum 8358 CPU @ 2.60GHz and 1.0 TB memory.

We assume attacks come either from external networks or existing files. Thus, we set their initial integrity score in A_0 to 0, which means low integrity, in compliance with our conservative settings mentioned in §IV-B.

We partition each dataset into training and testing sets, adhering to the assumption stated in §II-C that the training set should not contain any malicious activities. Specifically, we find out the first attack starting time from the ground truth. Then, all data produced prior to the first attack date becomes the training set, whereas the remaining data becomes the testing set. The duration and size of these training and testing sets are detailed in Table IX in the appendix.

3) *Baseline Detectors*: We compare CAPTAIN with five SOTA PIDS: FLASH [34], KAIROS [9], SHADEWATCHER [51], NODLINK [25], and MORSE [19] to evaluate their performance from different perspectives. We chose FLASH, KAIROS, and NODLINK because they are the most recent and SOTA embedding-based PIDS. In addition, their implementations are open-sourced, allowing us to test them on different datasets. Since some other embedding-based PIDS [45], [16], [30] have already been evaluated in [34], [9], [25] and the result shows that FLASH, KAIROS, and NODLINK outperform them, we didn’t include them in our evaluation. We chose MORSE since it is the SOTA rule-based PIDS, and we want to evaluate the improvements from our differentiable adaptation framework in CAPTAIN. According to [9], [34] and our communication with the authors, the detection systems of SHADEWATCHER and PROGRAPHER are not fully open-source due to proprietary license restrictions. Although the data preprocessing module of SHADEWATCHER is open-sourced, we tried our best but could not locate the preprocessing output files used for the following training and testing. We then realized that it was not feasible for us to

²<https://github.com/LexusWang/CAPTAIN>

perfectly replicate their systems for an unbiased comparison. Therefore, we used the code to evaluate the efficiency and latency of data preprocessing and the detection results reported in their paper to evaluate detection accuracy.

For FLASH, KAIROS, and NODLINK, we used their open-sourced code as the basis for the evaluation. We reimplemented MORSE according to their paper. All codes used for evaluating the baselines will also be publicly available for future research.

B. Detection Accuracy

In this section, we compare CAPTAIN with the SOTA PIDS in terms of the detection performance.

1) *False Alarm Events Reduction*: We first focus on the reduction of false alarm events, which requires the detector to have the detection granularity at the event level. We compare CAPTAIN with the SOTA event-level PIDS SHADEWATCHER and the classical tag-based PIDS MORSE. Due to the close-source nature of SHADEWATCHER, we used the reported detection results in their paper.

The results show that both MORSE and CAPTAIN successfully detected all attacks in the testing dataset. But CAPTAIN reduces the false alarm rate by over 93% (15.66x) compared to SHADEWATCHER and over 95% (20.45x) compared to MORSE. Additionally, SHADEWATCHER holds 80% of events for training and only 10% for testing, while the testing set of CAPTAIN is over seven times larger than the testing set of SHADEWATCHER. This shows that CAPTAIN doesn't require as much data as SHADEWATCHER for training.

TABLE III: Comparison with the baselines on the TRACE dataset from Engagement 3 in terms of false alarm events

	MORSE	SHADEWATCHER	CAPTAIN
# of Consumed Events	5,188,230	724,236	5,188,230
# of False Alarm Events	22,500	2,405	1,099
False Alarm Rate	0.434%	0.332%	0.0212%

One advantage of the rule-based PIDS like CAPTAIN and MORSE is that it can offer semantic-rich alarms, while SHADEWATCHER only flags deviations from patterns observed during training but doesn't explain the alarm. We then compared the number of false alarms generated by CAPTAIN and MORSE into different categories. The results are shown in Table IV.

Table IV shows that CAPTAIN can reduce false alarms by over 90% (11.49x) on average for all datasets compared with the non-adaptive MORSE. It outperforms MORSE in every alarm category. For those remaining false alarms, especially in C-5, S-2, and S-3, CAPTAIN cannot remove them by only learning the benign traces for the following reasons. First, some "false" alarms are not purely benign. They are related to some (potential) attack nodes (e.g., some configuration files in `/tmp/atScript/atomic-red-team-Gray_dev1.0/*` in S-2) but cannot be mapped to specific attack steps directly, so they are not labeled as "malicious." Second, some nodes and edges don't exist or trigger any alarm in the training set. Third, since we try to be as conservative as possible, some parameters are

tuned just enough to eliminate false alarms in the training set. However, in the testing set, these conservative settings can still cause false alarms again.

2) *False Alarm Entity Reduction*: While CAPTAIN operates as an event-level detector, we still compare CAPTAIN with the SOTA entity-level PIDS FLASH, KAIROS, and NODLINK (KAIROS and NODLINK give the result at graph-level, but they also support entity-level detection). We transformed the alarm events triggered by CAPTAIN into alarm entities using the following method: an entity is considered an alarm entity if it is involved in any alarm events.

It is noteworthy that only a subset of each DARPA dataset is utilized for training and testing in [45], [34], [9]. To simulate the real scenario in SOC, for each DARPA dataset, we utilize the entire dataset for evaluation, employing the method for dividing the training and testing sets as described in §VI-A2. We retrained the model and performed detection using their code. Additionally, we noticed FLASH and THREATTRACE did not count the FPs within the two-hop distance from the labeled attack entities in the ground truth while counting the TPs within the two-hop distance from the detected entities [9]. To ensure a fair comparison without providing excessive leniency, we report the TP and FP results, as well as the one-hop FP result, in which we exclude the FP entities within a one-hop distance from the ground truth. The aforementioned experiment settings and data labeling can explain the difference between our results and the results in their papers.

We evaluated the detection accuracy on CADETS, TRACE, and THEIA datasets of Engagement 3 since those datasets were commonly used by baselines. Table V illustrates the comparison among CAPTAIN and the baselines. On all datasets, CAPTAIN demonstrates superior performance in identifying more TPs while maintaining fewer FPs. FLASH can report a fair amount of TPs but produce an excessive amount of FPs. FLASH leverages GNN to learn k -hop neighborhood structures. While this technique shows promising performance when there is a significant anomaly within k -hop distance, it could degrade when the training set is limited [34]. We observed that although KAIROS also detected many anomalous entities, it can filter out FPs with the Anomalous Time Window Queue [9]. It guaranteed decent detection accuracy at the time-window level; the entity-level accuracy, however, is not satisfactory. NODLINK can detect all attack processes with a high number of FPs. Moreover, missing other relevant entities, such as files and network sockets, require additional efforts from security analysts to investigate the reported attacks.

CAPTAIN successfully detected all attacks in the dataset. Since CAPTAIN is an event-level detector, some entities that are not directly related to the attack events will not be reported. For example, if a malware is downloaded and executed, we report the MalFileCreation alarm and the FileExec alarm, which can give the analysts the malware process, file, and parent process. We do not immediately report the entry network node used by attackers to avoid alarm fatigue, which explains the FNs of CAPTAIN. The investigations on the relevant nodes can be conducted after the first response.

TABLE IV: Comparison with the baseline on different datasets regarding false alarms. We use T-3 and T-5 to represent the TRACE datasets from Engagement 3 and Engagement 5, as well as C-3 and C-5 to represent the CADETS datasets from Engagement 3 and Engagement 5. S-1 to S-3 denote SOC-Cloud, SOC-Streaming, and SOC-Dev datasets, respectively.

Datasets	FileExe		MemExec		ChPerm		Corrupt		DataLeak		Escalate		Total False Alarms		
	Base	Ours	Base	Ours	Base	Ours	Base	Ours	Base	Ours	Base	Ours	Base	Ours	Reduction
T-3	8	0	20.4K	1.08K	1	1	628	2	844	21	671	0	22.5K	1.10K	20.45x
C-3	41	14	N/A	N/A	8	8	13.3K	946	55	25	81	0	13.4K	993	13.49x
T-5	181	170	403K	79.8K	0	0	34.4K	19.9K	26.9K	1.20K	18.4K	28	483K	101K	4.78x
C-5	1.86K	198	N/A	N/A	N/A	N/A	1.95M	977K	8.58K	6.87K	1.45K	4.02K	1.97M	988K	1.99x
S-1	3.16K	0	N/A	N/A	26	0	100	73	22	21	N/A	N/A	3.31K	94	35.21x
S-2	177	53	N/A	N/A	0	0	12	9	14	7	N/A	N/A	203	69	2.94x
S-3	18	0	N/A	N/A	0	0	29	16	23	22	N/A	N/A	60	38	1.58x

TABLE V: Comparison with the baselines in terms of node-level detection accuracy

	TP	FP (0-hop)	FP (1-hop)	FN	TN
Engagement3 CADETS					
FLASH	24	29669	29633	10	2705545
KAIROS	4	1343	1279	30	2733871
NODLINK ¹	6	38248	38246	0	-
CAPTAIN	24	1137	1130	10	2734077
Engagement3 TRACE					
FLASH	8	133405	133364	14	176403042
NODLINK ¹	3	4782	4773	0	-
CAPTAIN	10	51	47	12	176536396
Engagement3 THEIA					
FLASH	2	129859	129800	18	6998697
KAIROS	2	3576	3569	18	7124980
NODLINK ¹	4	8743	8735	0	-
CAPTAIN	7	2684	2674	13	7125873

¹Since NODLINK only provides detected process, we evaluate it on process detection accuracy.

Another reason for missing TP is that we did not count the attack entities in the 2-hop neighborhood of the detected entities as TP like [34], [9], [45] did. This strict TP calculation method results in more FNs shown in this paper, but we believe it is necessary to assess the performance of PIDS in real-world scenarios.

C. Efficiency

1) *Detection Latency*: In previous sections, we introduced CAPTAIN’s rule-based detection framework, highlighting its simplicity compared to other embedding-based PIDS. In this section, we compare CAPTAIN with the SOTA PIDS FLASH, KAIROS, NODLINK, and SHADEWATCHER to evaluate their response latency. Our latency analysis encompasses three dimensions: **buffer time**, **preprocessing time**, and **detection time**.

We have already introduced buffer time in II-A. Preprocessing time refers to the duration taken to convert the raw audit logs into a data structure that the detection systems can process. It involves data parsing, data cleaning, noise reduction, preprocessing, feature extraction, and so on.

Detection time refers to the interval between the completion of data processing and the moment the result is produced. It is noteworthy that since the detection granularity is different in different PIDS, the detection time might not reflect the actual

latency of each system. For instance, a detector based on the whole graph may take longer to deliver detection results of each graph compared with a detector on the entity/event level. However, this does not necessarily mean the former is slower because a large graph could contain many entities and events. Therefore, we calculate the total time spent on detection across the entire dataset.

We use the TRACE and CADETS data from DARPA Engagement 3 as the representative datasets for the latency evaluation since they covered all baselines. Since the training stage can be conducted offline, our evaluation focused on these metrics within the context of the testing set. We minimized the bias in our evaluation. For example, FLASH divided the data processing into two stages in their code and used files to store intermediate results. And KAIROS employed the PostgreSQL database in their code and some files to store the intermediate results. These are the steps not required in a real-time streaming pipeline. Consequently, we excluded the I/O time to focus solely on measuring the “pure” preprocessing and detection time.

The result is shown in Table VI. Unlike other PIDS that rely on embedding the graph structure and require a buffer time ranging from several minutes to several hours, CAPTAIN processes audit logs in a streaming fashion, eliminating the need for any buffer time. CAPTAIN is also faster in preprocessing because the logs do not need much preparation for the machine learning model. Because the tags of CAPTAIN are much simpler than the state vectors used by FLASH and KAIROS, and we avoid using text embedding or GNN to aggregate the semantic and contextual graph information, CAPTAIN is over 10x faster than the baselines in detection.

2) *Runtime Overhead*: Another important metric reflecting the efficiency of a PIDS is the runtime overhead to the system. In this section, we evaluated the runtime overhead of CAPTAIN during detection and conducted a comparative study with other SOTA PIDS. We also analyzed the memory consumption of CAPTAIN during the training stage.

Runtime Overhead in Detection: We used the Python `resource` module to evaluate detectors’ resource consumption. We ran the detectors on CPU mode. As admitted in [51], GPUs may not be available in most real-life threat detection scenarios. We calculated the total CPU time in user mode to evaluate the CPU resource consumption. The result is shown

TABLE VI: Comparison of detection latency

	Buffer Time	Preprocessing Time	Detection Time
Engagement3 TRACE			
FLASH	57:49	107:50	64:24
SHADEWATCHER	N/A ¹	100:22	3:40 ²
NODLINK	00:10	135:42	2:48
CAPTAIN	0	58:20	5:11
Engagement3 CADETS			
KAIROS	15:00	15:34	29:46
FLASH	82:52	18:57	7:41
NODLINK	00:10	6:18	6:41
CAPTAIN	0	7:22	1:23

¹We did not find a clear number in their paper or codes.

²SHADEWATCHER extracts the last 10% interactions as the testing set, while the testing set of us is around 2.5 times larger.

in Fig. 4a. Please note that the total CPU time used in Fig. 4a could be more than the detection time in Table VI because of the multi-core usage of CPU in the deep learning module. Since CAPTAIN only relies on straightforward arithmetic operations on real-number tags, it requires significantly less CPU time than the embedding-based PIDS (around 2% of FLASH and around 0.02% of KAIROS), which need complex matrix and vector operations due to their use of neural networks.

We used the `psutil` library in Python to monitor the live memory usage of the detectors. The comparison of memory usage over time for detection is shown in Fig 4b. Compared to the baselines, CAPTAIN finishes detection much faster than the baselines (as we have already seen in Table VI) and achieves the lowest memory usage throughout the entire detection process.

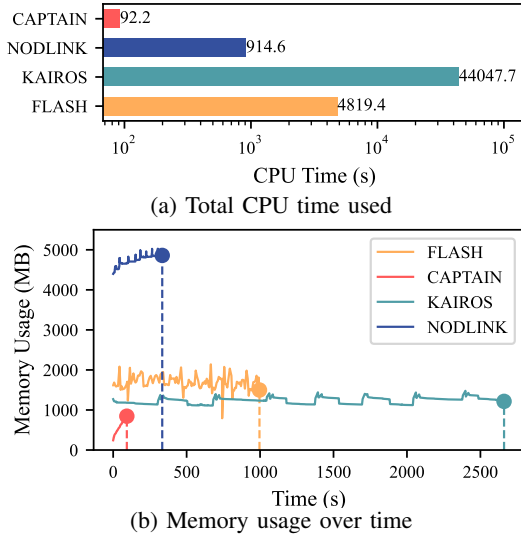


Fig. 4: Comparison of resource consumption when detecting on DARPA Engagement 3 CADETS

Runtime Overhead in Training: In real-world scenarios, the training stage of the detection system can be performed offline, where users can allocate ample time and computing resources, including GPUs. Therefore, we did not evaluate the runtime overhead and the time used for training. However, as CAPTAIN records and propagates the gradients for each

tag among the big graph, a reasonable concern is that saving those gradients would consume much memory when there is a dependency explosion problem. Our evaluation shows that, in practice, we would not need so much space because most gradients would always be zero since the provenance graph is a sparse graph. We evaluated the number of non-zero gradients that CAPTAIN needs to save during training. The results, shown in Fig. 8, illustrate that most nodes only need to store a small number of gradients during training. Due to the space limit, the detailed results can be found in § C-B.

D. Resilience Against Adversarial Attacks

As more PIDS have been developed to analyze provenance data, adversarial attacks aimed at evading these provenance-based detection mechanisms have garnered more attention. In this section, we discuss the robustness of CAPTAIN against two main-stream adversarial attacks: adversarial mimicry attack and dataset poisoning attack.

1) *Adversarial Mimicry Attack:* Mimicry attacks on PIDS involve altering the provenance data and incorporating more benign features to "mimic benign behavior", thereby evading detection. In this section, we evaluated the robustness of CAPTAIN against mimicry attacks using the attack methodology in [15], [34], i.e. inserting benign structures into the attack graphs. Our mimicry attack contains two steps. First, we extract some events of benign system entities from the normal training data. Then we add some "fake" events where we replace the benign system entities with the attack entity to simulate the attack entity doing similar activities as the benign entities. To verify the effectiveness of our mimicry attack, we also use FLASH as the baseline.

For evaluation purposes, we used the CADETS dataset in Engagement 3 as the example because of its relatively small scale. The details about our mimicry experiment can be found in the Appendix C-C. The result is shown in Fig. 5.

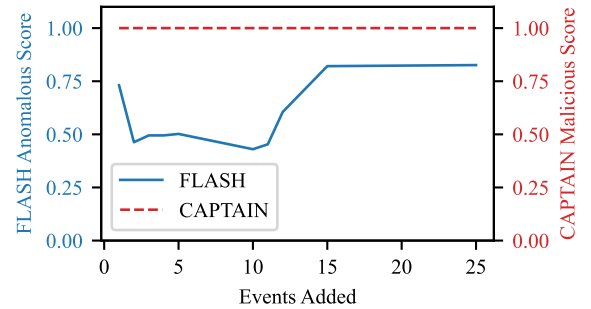


Fig. 5: Adversarial mimicry attack against CAPTAIN and FLASH (use the attack entity `/tmp/test` as an example)

In general, both CAPTAIN and FLASH showed robustness against our mimicry attack attempt to some extent. The attack entity `/tmp/test` is still detected by both systems even after we add some normal activities. However, we can see a significant drop in the anomalous score of FLASH when we introduce a relatively small number of events (fewer than 10), which is also confirmed in their paper [34]. On the other

hand, CAPTAIN remains unaffected by the mimicry attack, demonstrating superior robustness compared to the baseline.

The robustness of CAPTAIN results from three main reasons. First of all, the propagation of CAPTAIN is guided by heuristic-based rules, while the propagation and aggregation of FLASH and other embedding-based PIDS are based on the neural network. Second, CAPTAIN is an event-level detector with a finer granularity than entity-level detectors. As mentioned before, CAPTAIN gives the detection result for each streaming event without any buffer time, which means any mimicry insertion after the real attack activities is useless. For those PIDS that need a buffer time, any events within the same time window or related to the same entity can affect the final detection result. Third, CAPTAIN is not an anomaly-based detector. In other words, the detection is performed based on the conservative, heuristic rules, while the normal data is only used to reduce the false alarms. Therefore, adding normal features can not compromise the detection capability as it is guaranteed by the conservative detection rules.

2) *Traning Set Poisoning Attack*: Dataset poisoning refers to the malicious manipulation on the training set that is relied on by the learning system. In the context of cyber security and intrusion detection, it usually involves polluting the benign training set with adversarial events/entities. When the detector is trained on a "benign" dataset that has been polluted, it learns patterns or features introduced by attackers. These patterns and features, once learned, could assist attackers in evading detection in future instances.

We add a regularizer term to the loss function to control the sensitivity of CAPTAIN to the training set. This enhances CAPTAIN's robustness against dataset poisoning attacks.

We evaluated this robustness using a specific real example of Pine Backdoor & Phishing Email attack from T-3. In this attack, a vulnerable `pine` connected to the C2 server `128.55.12.73` and executed an email attachment. However, IP `128.55.12.73` had multiple activities and caused some "false" alarms in the training set. Please note that this violates our assumption stated in § II-C that the training set must not be compromised by malicious entities or events. Nevertheless, this makes it a perfect example to test the robustness against data poisoning attacks.

Table VII shows the values of two critical parameters in detecting this attack: the initial integrity tag of `128.55.12.73` and the tag propagation rate of event (`pine, read, 128.55.12.73`), under different learning settings. We use the conservative setting (A_0 , G_0 , and T_0) as the baseline. The result illustrates that if we don't use the regularization term, `128.55.12.73` will be treated as a pure benign IP, and the propagation rate to the process `pine` is 0, which lets us miss the attack. With the increase of the regularizer coefficients, CAPTAIN is more cautious when learning the training data. Finally, we successfully captured this special attack with a larger regularizer coefficient. In practice, the regularizer coefficients can be set based on the confidence in the training data, the tolerance to the missing alarm, and the trade-off between TP and FP.

TABLE VII: Case study on the effectiveness of the regularization term in the loss function.

	Base	The value of α, λ, τ		
		0	10	100
$a_{(128.55.12.73)}$	0	1.00	0.818	0.391
$g(pine, read, 128.55.12.73)$	1	0.980	0.985	0.992
Detected?	Yes	No	No	Yes

E. Ablation Study

1) *Individual Adaptive Parameters*: We conduct an ablation study on each adaptive parameter, comparing the detection performance with or without specific adaptive parameters. As each parameter can be learned and adjusted independently, we have seven separate experiments, each optimizing a different subset of the parameters, i.e. $\{A\}$, $\{G\}$, $\{T\}$, $\{A, G\}$, $\{A, T\}$, $\{G, T\}$, and $\{A, T, G\}$.

According to the experiments, adjusting the threshold (T) alone may not have much effect on the detection results because when the initial tags and the propagation rates are unchanged, the tags after the propagation also tend to be 0 or 1. Therefore, tuning a continuous threshold would not influence the final alarm decision. It should be noted that tuning A plays the most major role in mitigating false alarms among these three adaptive parameters. In other words, tuning the initial tags of nodes can help filter out the false alarms more than tuning the propagation rates and the thresholds.

While tuning parameters A , G , and T together often yields incremental improvements, adjusting A alone sometimes results in fewer false alarms in certain datasets (S-3 and C-3). This is because, without the benefit of adjusting the propagation rate and the threshold, we have to assign higher integrity tags to more nodes to counteract false alarms in training sets. Although this can reduce false alarms more crudely and simply, it also carries the risk of being excessively lenient, which might be hazardous in some contexts.

Another advantage of tuning all these three parameters is that it can accelerate the training process. This is shown in Fig.6. Although $\{A\}$, $\{A, T\}$, and $\{A, T, G\}$ achieve similar good detection results on the testing set, $\{A, T, G\}$ converges using fewer epochs during training.

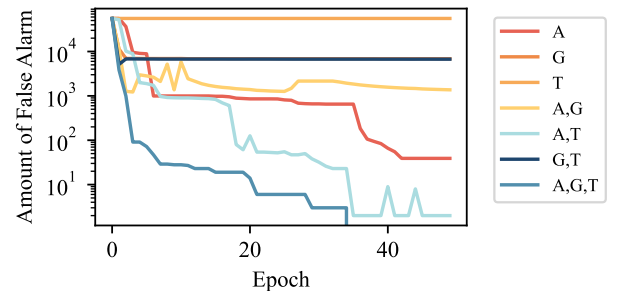


Fig. 6: Ablation study on each parameter.

2) *Learning Rate in Optimization*: During training, the learning rate is a critical hyperparameter that not only determines the learning speed but also controls the granularity of

the search. We conducted an experiment on different learning rates on the DARPA Engagement 3 CADETS data. The detailed results can be found in § C-D. As illustrated in Fig. 9, a higher learning rate usually leads to a sharper loss decline during the initial training epochs. However, for ongoing training, a lower learning rate may yield a finer-tuned search process and lower loss. In cases where training time on large graphs is a critical factor, a balance between training speed and training quality may be necessary.

F. Case Study

To explore the explainability of CAPTAIN, we delve into the training outcomes of the E3-TRACE dataset as a case study.

Tag Initialization (A) Adjustments: Examining the parameters in A , the adjustments from A_0 primarily focused on network objects, showcasing a broad spectrum of modifications. Notably, internal IP addresses, such as 128.55.12.10, 128.55.12.122 and 128.55.12.73, were assigned initial integrity values close to 1. Other IP addresses, like 65.214.39.18 and 216.9.245.101, are assigned initial integrity values around 0.5. Additionally, certain IP addresses, such as 208.17.90.11 and 162.93.202.80, were endowed with initial integrity values slightly exceeding 0. The discrepancies in the learned integrity values reflect the varying levels of trust CAPTAIN places in these IP addresses. Internal IP addresses, in particular, triggered numerous alarms through potentially malicious behaviors during the training period. To reduce such false alarms, CAPTAIN learned to trust these internal IP addresses, leading to the assignment of elevated integrity values. Other IP addresses, appearing less frequently and engaging in less sensitive activities, received neutral integrity values. Moreover, some IP addresses, despite participating in sporadic sensitive activities eventually deemed benign, did not garner significant trust from CAPTAIN. Consequently, their initial integrity values underwent a minimal change from A_0 . Compared with manual whitelisting, CAPTAIN can assign integrity with finer granularity, allowing it to navigate the trade-offs between true positives and false positives more effectively.

Propagation Rate (G) Adjustments: Examining the parameters in G , the adjustments from G_0 predominantly focus on read and write operations on files. Notably, events involving `bash` reading from `.bash_history` received a relatively low propagation rate, approximately 0.5, while other events associated with `.bash_history` maintained a high propagation rate close to 1. As discussed in § III, `bash` frequently engages in reading and writing activities with `.bash_history` during routine tasks, potentially causing dependency explosions and triggering numerous false alarms. Through the training process, CAPTAIN learned to mitigate false positives by reducing the propagation rates for events involving `bash` reading from `.bash_history`. Meanwhile, CAPTAIN remained cautious with other `.bash_history` related events, maintaining relatively high propagation rates to ensure malicious intent can still propagate through alternative pathways. The fine-grained adjustment of propagation rates

by CAPTAIN diminishes false positives while preserving its robustness, thereby preventing attackers from easily evading detection.

Alarm Generation Threshold (T) adjustments: Upon scrutinizing the parameters in T , the adjustments encompass various events capable of triggering alarms. Notably, we observed that the threshold for generating data leak alarms is set close to 0 for processes such as `sshd`, `thunderbird`, and `firefox` when they send messages to internal IP addresses. In contrast, the threshold for generating data leak alarms when these processes send messages to other IP addresses remains around the default value of 0.5. Furthermore, the internal IP addresses associated with these processes are distinct. For instance, `sshd` exhibits a low alarm generation threshold exclusively when sending messages to 128.55.12.122 and 128.55.12.10, while `thunderbird` displays a low threshold when communicating with 128.55.12.73. These observations indicate that CAPTAIN has effectively learned to diminish false alarms by lowering the threshold for generating such alarms at the edge level. These adjustments are finely tuned to specific processes communicating with particular IP addresses, while leaving the alarm generation threshold unaltered for other processes communicating with these IP addresses or for these processes communicating with other IP addresses. This fine-grained and nuanced approach not only allows CAPTAIN to effectively reduce false alarms but also fortifies it against living-off-the-land attacks that seek to emulate benign activities. The resilience to such attacks persists unless the attackers can successfully gain access to the internal IP addresses featured in the training dataset, thereby significantly heightening the complexity and challenge of executing such an attack.

VII. DISCUSSION AND FUTURE WORK

A. More Optimization Algorithms

In this paper, we utilize the gradient descent algorithm for optimization because of its simplicity and clearness. There are more gradient-based optimization algorithms. We discuss their applicability based on our differentiable tag propagation framework in this section. In fact, we used *Batch gradient descent* in CAPTAIN. The batch size is fixed to the number of events in each dataset. Using a smaller batch size means updating the adaptive parameters before finishing a single round of detection, which could cause tag inconsistency in a single provenance graph. Instead of directly updating parameters based on the gradients, we can modify these gradients to reach optimal values more quickly and accurately, using algorithms such as *Nesterov Accelerated Gradient (NAG)* [31], *Adadelta* [49], *RMSprop*, *Adagrad* [14], *Adam* [21], *AdaMax*, *Nadam*, and so on. These algorithms require the first-order gradient, which is offered by the differentiable tag-propagation framework in CAPTAIN. We leave the implementation of these algorithms as the extensions of CAPTAIN.

B. Online Learning

We assess CAPTAIN in an offline setting for automatic data labeling. However, the architecture of the detection and

learning modules doesn't preclude the use of CAPTAIN in an online setting with manual labeling. Specifically, CAPTAIN's learning module can compute loss upon receiving manually determined false alarms. Subsequently, the learning module can promptly update the adaptive parameters for subsequent detection.

VIII. CONCLUSION

This paper introduces CAPTAIN, a tag-based PIDS capable of automatically adapting to diverse detection environments. CAPTAIN's flexibility, enhanced by three adaptive parameters: tag initialization (A), propagation rate (G), and threshold (T), distinguishes it from existing rule-based PIDS. We have developed a differentiable tag propagation framework that records gradients, enabling the optimization of these parameters using the gradient descent algorithm. To our knowledge, this is the first effort to incorporate gradient descent methods in optimizing rule-based PIDS. We then evaluate CAPTAIN using several APT attack datasets. Our results demonstrate a remarkable capability of CAPTAIN to adapt to different environments automatically, significantly reducing false alarms, detection latency, and runtime overhead, outperforming the SOTA baselines.

REFERENCES

- [1] B. A. Alahmadi, L. Axon, and I. Martinovic, "99% false positives: A qualitative study of SOC analysts' perspectives on security alarms," in *31st USENIX Security Symposium (USENIX Security 22)*. Boston, MA: USENIX Association, Aug. 2022, pp. 2783–2800. [Online]. Available: <https://www.usenix.org/conference/usenixsecurity22/presentation/alahmadi>
- [2] A. Alsaheel, Y. Nan, S. Ma, L. Yu, G. Walkup, Z. B. Celik, X. Zhang, and D. Xu, "Atlas: A sequence-based learning approach for attack investigation," in *USENIX Security Symposium*, 2021, pp. 3005–3022.
- [3] A. Alshamrani, S. Myneni, A. Chowdhary, and D. Huang, "A survey on advanced persistent threats: Techniques, solutions, challenges, and research opportunities," *IEEE Communications Surveys Tutorials*, vol. 21, no. 2, 2019.
- [4] S. Arzt, S. Rasthofer, C. Fritz, E. Bodden, A. Bartel, J. Klein, Y. Le Traon, D. Octeau, and P. McDaniel, "Flowdroid: Precise context, flow, field, object-sensitive and lifecycle-aware taint analysis for android apps," *ACM sigplan notices*, vol. 49, no. 6, pp. 259–269, 2014.
- [5] K. Bandla, "Apt notes," 2019. [Online]. Available: <https://github.com/kbandla/APTnotes>
- [6] R. Canary, "Explore atomic red team," 2023. [Online]. Available: <https://atomicredteam.io/>
- [7] V. Chandola, A. Banerjee, and V. Kumar, "Anomaly detection: A survey," *ACM Comput. Surv.*, vol. 41, no. 3, jul 2009. [Online]. Available: <https://doi.org/10.1145/1541880.1541882>
- [8] Y. Chen, Y. Chi, J. Fan, and C. Ma, "Gradient descent with random initialization: Fast global convergence for nonconvex phase retrieval," *Mathematical Programming*, vol. 176, pp. 5–37, 2019.
- [9] Z. Cheng, Q. Lv, J. Liang, Y. Wang, D. Sun, T. Pasquier, and X. Han, "Kairos: Practical intrusion detection and investigation using whole-system provenance," *arXiv preprint arXiv:2308.05034*, 2023.
- [10] CISA, "North korean advanced persistent threat focus: Kimsuky," 2020. [Online]. Available: <https://www.cisa.gov/uscert/ncas/alerts/aa20-301a>
- [11] S. C. Committee, "A 'kill chain' analysis of the 2013 target data breach," 2014. [Online]. Available: <https://www.commerce.senate.gov/services/files/24d3c229-4f2f-405d-b8db-a3a67f183883>
- [12] C. Dietrich, K. Krombholz, K. Borgolte, and T. Fiebig, "Investigating system operators' perspective on security misconfigurations," in *Proceedings of the 2018 ACM SIGSAC Conference on Computer and Communications Security*, ser. CCS '18. New York, NY, USA: Association for Computing Machinery, 2018, p. 1272–1289. [Online]. Available: <https://doi.org/10.1145/3243734.3243794>
- [13] F. Dong, S. Li, P. Jiang, D. Li, H. Wang, L. Huang, X. Xiao, J. Chen, X. Luo, Y. Guo *et al.*, "Are we there yet? an industrial viewpoint on provenance-based endpoint detection and response tools," in *Proceedings of the 2023 ACM SIGSAC Conference on Computer and Communications Security*, 2023, pp. 2396–2410.
- [14] J. Duchi, E. Hazan, and Y. Singer, "Adaptive subgradient methods for online learning and stochastic optimization," *Journal of machine learning research*, vol. 12, no. 7, 2011.
- [15] A. Goyal, X. Han, G. Wang, and A. Bates, "Sometimes, you aren't what you do: Mimicry attacks against provenance graph host intrusion detection systems," in *30th Network and Distributed System Security Symposium (NDSS 23)*, 2023.
- [16] X. Han, T. F. J. Pasquier, A. Bates, J. Mickens, and M. I. Seltzer, "Unicorn: Runtime provenance-based detector for advanced persistent threats," in *27th Annual Network and Distributed System Security Symposium, NDSS 2020, San Diego, California, USA, February 23-26, 2020*. The Internet Society, 2020. [Online]. Available: <https://www.ndss-symposium.org/ndss-paper/unicorn-runtime-provenance-based-detector-for-advanced-persistent-threats/>
- [17] W. U. Hassan, S. Guo, D. Li, Z. Chen, K. Jee, Z. Li, and A. Bates, "Nodoze: Combatting threat alert fatigue with automated provenance triage," in *26th Annual Network and Distributed System Security Symposium, NDSS 2019, San Diego, California, USA, February 24-27, 2019*. The Internet Society, 2019. [Online]. Available: <https://www.ndss-symposium.org/ndss-paper/nodoze-combatting-threat-alert-fatigue-with-automated-provenance-triage/>
- [18] M. N. Hossain, S. M. Milajerdi, J. Wang, B. Eshete, R. Gjomemo, R. Sekar, S. Stoller, and V. Venkatakrishnan, "{SLEUTH}: Real-time attack scenario reconstruction from {COTS} audit data," in *26th USENIX Security Symposium (USENIX Security 17)*, 2017, pp. 487–504.
- [19] M. N. Hossain, S. Sheikhi, and R. Sekar, "Combating dependence explosion in forensic analysis using alternative tag propagation semantics," in *IEEE Symposium on Security and Privacy (SP)*, 2020.
- [20] S. S. Khan and M. G. Madden, "One-class classification: taxonomy of study and review of techniques," *The Knowledge Engineering Review*, vol. 29, no. 3, pp. 345–374, 2014.
- [21] D. P. Kingma and J. Ba, "Adam: A method for stochastic optimization," *arXiv preprint arXiv:1412.6980*, 2014.
- [22] F. B. Kokulu, A. Soneji, T. Bao, Y. Shoshitaishvili, Z. Zhao, A. Doupe, and G.-J. Ahn, "Matched and mismatched socs: A qualitative study on security operations center issues," in *Proceedings of the 2019 ACM SIGSAC conference on computer and communications security*, 2019, pp. 1955–1970.
- [23] T. R. Lampert, "CHAOS: a PoC that allow generate payloads and control remote operating systems. Features like persistency and others can be achieved with a program updating and using the Dnsmaq service, which is also a feature of chaos." <https://github.com/tiagorlampert/CHAOS>, Year the repository was last updated.
- [24] K. H. Lee, X. Zhang, and D. Xu, "High accuracy attack provenance via binary-based execution partition." in *NDSS*, vol. 16, 2013.
- [25] S. Li, F. Dong, X. Xiao, H. Wang, F. Shao, J. Chen, Y. Guo, X. Chen, and D. Li, "Nodlink: An online system for fine-grained apt attack detection and investigation," *arXiv preprint arXiv:2311.02331*, 2023.
- [26] Z. Li, Q. A. Chen, R. Yang, Y. Chen, and W. Ruan, "Threat detection and investigation with system-level provenance graphs: a survey," *Computers & Security*, vol. 106, p. 102282, 2021.
- [27] S. Ma, X. Zhang, and D. Xu, "Protracer: Towards practical provenance tracing by alternating between logging and tainting," in *23rd Annual Network And Distributed System Security Symposium (NDSS 2016)*. Internet Soc, 2016.
- [28] J. R. Martins and A. Ning, *Engineering design optimization*. Cambridge University Press, 2021.
- [29] S. M. Milajerdi, B. Eshete, R. Gjomemo, and V. Venkatakrishnan, "Poirot: Aligning attack behavior with kernel audit records for cyber threat hunting," *ACM SIGSAC Conference on Computer and Communications Security*, 2019.
- [30] S. M. Milajerdi, R. Gjomemo, B. Eshete, R. Sekar, and V. Venkatakrishnan, "Holmes: Real-time apt detection through correlation of suspicious information flows," in *IEEE Symposium on Security and Privacy (SP)*, 2019.
- [31] Y. Nesterov, "A method for unconstrained convex minimization problem with the rate of convergence $O(1/k^2)$," in *Dokl. Akad. Nauk. SSSR*, vol. 269, no. 3, 1983, p. 543.

- [32] J. Newsome and D. X. Song, "Dynamic taint analysis for automatic detection, analysis, and signature generation of exploits on commodity software," in *NDSS*, vol. 5. Citeseer, 2005, pp. 3–4.
- [33] D. T. program, "Transparent Computing Engagement 3 Data Release," 2020. [Online]. Available: <https://github.com/darpa-i2o/Transparent-Computing/blob/master/README-E3.md>
- [34] M. U. Rehman, H. Ahmadi, and W. U. Hassan, "Flash: A comprehensive approach to intrusion detection via provenance graph representation learning," in *2024 IEEE Symposium on Security and Privacy (SP)*. IEEE Computer Society, 2024, pp. 139–139.
- [35] H. B. Review, "Missed alarms and 40 million stolen credit card numbers: How target blew it," <https://hbr.org/2014/03/could-target-have-prevented-its-security-breach>. [Online]. Available: <https://hbr.org/2014/03/could-target-have-prevented-its-security-breach>
- [36] H. Robbins and S. Monro, "A stochastic approximation method," *The annals of mathematical statistics*, pp. 400–407, 1951.
- [37] S. Ruder, "An overview of gradient descent optimization algorithms," *arXiv preprint arXiv:1609.04747*, 2016.
- [38] G. P. Spathoulas and S. K. Katsikas, "Using a fuzzy inference system to reduce false positives in intrusion detection," in *2009 16th International Conference on Systems, Signals and Image Processing*, 2009, pp. 1–4.
- [39] S. C. Sundaramurthy, A. G. Bardas, J. Case, X. Ou, M. Wesch, J. McHugh, S. R. Rajagopalan, and L. F. Cranor, "A human capital model for mitigating security analyst burnout," in *Eleventh Symposium On Usable Privacy and Security (SOUPS 2015)*, 2015, pp. 347–359.
- [40] D. M. Tax and R. P. Duin, "Data domain description using support vectors," in *ESANN*, vol. 99, 1999, pp. 251–256.
- [41] —, "Support vector domain description," *Pattern recognition letters*, vol. 20, no. 11-13, pp. 1191–1199, 1999.
- [42] N. Y. Times, "Equifax says cyberattack may have affected 143 million the u.s." <https://www.nytimes.com/2017/09/07/business/equifax-cyberattack.html>. [Online]. Available: <https://www.nytimes.com/2017/09/07/business/equifax-cyberattack.html>
- [43] Q. Wang, W. Hassan, D. Li, K. Jee, X. Yu, K. Zou, J. Rhee, Z. Chen, W. Cheng, C. Gunter, and H. Chen, "You are what you do: Hunting stealthy malware via data provenance analysis," 01 2020.
- [44] Q. Wang, W. U. Hassan, D. Li, K. Jee, X. Yu, K. Zou, J. Rhee, Z. Chen, W. Cheng, C. A. Gunter *et al.*, "You are what you do: Hunting stealthy malware via data provenance analysis," in *NDSS*, 2020.
- [45] S. Wang, Z. Wang, T. Zhou, H. Sun, X. Yin, D. Han, H. Zhang, X. Shi, and J. Yang, "Threatrace: Detecting and tracing host-based threats in node level through provenance graph learning," *IEEE Transactions on Information Forensics and Security*, vol. 17, pp. 3972–3987, 2022.
- [46] C. Xiong, T. Zhu, W. Dong, L. Ruan, R. Yang, Y. Cheng, Y. Chen, S. Cheng, and X. Chen, "Conan: A practical real-time apt detection system with high accuracy and efficiency," *IEEE Transactions on Dependable and Secure Computing*, vol. 19, no. 1, pp. 551–565, 2022.
- [47] W. Xu, S. Bhatkar, and R. Sekar, "Taint-enhanced policy enforcement: A practical approach to defeat a wide range of attacks," in *USENIX Security Symposium*, 2006, pp. 121–136.
- [48] F. Yang, J. Xu, C. Xiong, Z. Li, and K. Zhang, "{PROGRAPHER}: An anomaly detection system based on provenance graph embedding," in *32nd USENIX Security Symposium (USENIX Security 23)*, 2023, pp. 4355–4372.
- [49] M. D. Zeiler, "Adadelata: an adaptive learning rate method," *arXiv preprint arXiv:1212.5701*, 2012.
- [50] J. Zeng, Z. L. Chua, Y. Chen, K. Ji, Z. Liang, and J. Mao, "Watson: Abstracting behaviors from audit logs via aggregation of contextual semantics," in *NDSS*, 2021.
- [51] J. Zeng, X. Wang, J. Liu, Y. Chen, Z. Liang, T.-S. Chua, and Z. L. Chua, "Shadewatcher: Recommendation-guided cyber threat analysis using system audit records," in *2022 IEEE Symposium on Security and Privacy (SP)*. IEEE, 2022, pp. 489–506.
- [52] M. Zipperle, F. Gottwalt, E. Chang, and T. Dillon, "Provenance-based intrusion detection systems: A survey," *ACM Comput. Surv.*, vol. 55, no. 7, dec 2022. [Online]. Available: <https://doi.org/10.1145/3539605>

APPENDIX A

ATTACK SCENARIOS IN DATASETS

A. DARPA Engagement

E3-TRACE contains five attack attempts. In the first attempt, Firefox on the target host is exploited by visiting a malicious

website. The attackers then uploaded a payload and obtained a remote shell with root privilege. We will refer to this attack later as **Firefox Backdoor**. In the second attempt, the attackers sent a phishing e-mail with a link to a website hosted by the attackers. The victim entered the requested information on the website, and the attackers received the victim's personal information. This attack only involves network activities, and the malicious part is not visible in the audit data. We only know the victim visited an external website, which is a common activity. Thus, we removed this attack from our evaluation. In the third attempt, the attackers tried to exploit the target with a malicious browser extension but failed to connect to the target. Thus, we didn't include this attempt in our evaluation. The fourth attempt continues the previous attempt of the malicious browser extension exploitation. This time, the attacker successfully obtained a remote shell. Then, they wrote and executed a malicious executable to perform portscan. We will refer to this attack later as **Pine Backdoor**. The fifth attempt involves a phishing e-mail with executable attachments. The victim downloaded and executed the malicious executable; hence, the attackers obtained a remote console and performed a port scan on the target host. We will refer to this attack later as **Executable Attachment**.

Besides TRACE, we also analyzed attack campaigns in E3-CADETS dataset. There are four attack attempts made using the same technique. Three out of four attempts failed, so we only included the successful one in our evaluation. In this attempt, the Nginx web server was exploited with a malformed HTTP request, and the attackers gained access to a remote shell. Then, the attackers downloaded a malicious payload, which connected back to the attackers' listener to establish a persistent connection. The attackers also used the payload to perform a port scan. We will refer to this attack later as **Nginx Backdoor**.

B. Simulated Environments

The simulated APT attack chains are generated with our automated attack simulator. The automated attack generator is derived from the Atomic Red Team project [6], a library of atomic attacks mapped to the MITRE ATT&CK framework. We modified it so we can either determine or randomly select an atomic attack to execute at each attack stage and thus generate an attack chain from the individual tests. When we design the screenplay for simulated attacks, we leave most of the stages to be randomly selected to avoid manually introduced bias.

We designed three kinds of simulated attacks, including fully randomized, partially randomized, and deterministic attacks, to demonstrate the adaptability of our model. Each step in a fully randomized attack is randomly selected from the Atomic Red Team atomic attack library. A partially randomized attack has determined steps at some stages but randomly chooses steps for the rest of the steps. A deterministic attack has defined steps at every attack stage. We used one deterministic attack, the North Korean APT Kimsuky (Kim), and 3 partially randomized attacks, comprising a reverse shell attack

TABLE VIII: Dataset Details

Dataset	OS	Duration(hh:mm)	# of Nodes	# of Events	Attacks
E3-TRACE	Linux	263:05	14.10M	20.86M	Firefox Backdoor, Pine Backdoor, Phishing Email
E3-THEIA	Linux	247:02	1.587M	27.47M	Firefox Backdoor, Browser Extension, Phishing E-mail
E3-CADETS	FreeBSD	263:28	614.5K	8.127M	Nginx Backdoor
E5-TRACE	Linux	248:23	173.6M	1596M	Firefox Elevate Inject, Nmap Scan
E5-CADETS	FreeBSD	249:05	14.13M	1194M	Nginx Backdoor, Nmap Scan
SOC-Streaming	Linux	06:51	302.9K	1.731M	ReverseShell, WebShell, AttackChain, Kimsuky, Chaos
SOC-Dev	Linux	06:32	78.89K	187.1K	ReverseShell, WebShell, AttackChain, Kimsuky, Chaos
SOC-Cloud	Linux	06:42	2.464M	5.817M	ReverseShell, AttackChain, Kimsuky, Chaos

TABLE IX: Training and testing time for each dataset. The dataset durations are in the format (*hh : mm*). The dataset size is denoted by the number of events.

Dataset	Training		Testing	
	Dur.	Size	Dur.	Size
T-3	174:55	15.7M	88:10	5.2M
C-3	77:53	1.9M	185:36	5.4M
T-5	70:45	119.6M	177:38	312.0M
C-5	71:15	59.8M	177:50	208.8M
S-1	5:23	8.5M	1:28	3.6M
S-2	5:01	1.2M	1:31	629K
S-3	5:13	209.0K	1:29	113K

(RS), a web shell attack (WS), and a payload attack (Chaos) in our evaluation. Kimsuky is an active APT group based in North Korea. We refer to a threat intelligence report[10] to select techniques used in each attack stage and reproduce North Korean APT Kimsuky with the help of Atomic Red Team[6]. The reverse shell, the web shell, and the payload attack uploaded three different payloads to establish the connection between the target host and the attackers to complete the attack. Finally, we also generated fully randomized attack chains (AC) using Atomic Red Team for the evaluation.

As for the benign scenarios, the SOC provided a list of detailed operation environments in the real world. Since some operation environments have similar configurations, we selected a subset of rather distinguished environments to reproduce. When we select scenarios to simulate, we also intentionally include applications and services that often trigger false alarms. Eventually, we reproduced three representative environments. Streaming simulates a data store and streaming server. Dev simulates a development server. Cloud simulates a cloud server. Table X specifies the apps or processes running in each simulated environment.

Once we have the simulated attacks and operation environments, we conduct the experiments following the attack campaign pattern used in DARPA Engagements to make it as realistic as possible. We start the data collector in three simulated environments and keep it running for a day. During the day, we ask a red team to perform attacks on all three targets at some time. In the end, we have the data produced in a day from 3 hosts and the ground truth of attacks performed. Table VIII summarizes the information of the three datasets

we collected in the described manner.

APPENDIX B CAPTAIN POLICIES

A. Tag Propagation Policies

We adopted tag propagation policies from MORSE [19] in our implementation. The tag propagation policies are detailed in Table XI. In the table, *dtag* refers to the data tag and *ptag* refers to the code tag. T_{qb} and T_{qe} stand for quiescent tag values for benign and suspect environment processes. d_b and d_e are decay rates for benign and suspect environment processes. a_b and a_e are the attenuation factors for benign and suspect environment subjects. Please refer to the original paper for formal and detailed definitions of these parameters. To get a fair comparison, we set all hyperparameters in Table XI as the default values according to the recommendation in the original paper.

B. Alarm Generation Policies

We adopted alarm generation policies from MORSE [19] in our implementation. The alarm generation policies are detailed in Table XII. *incl_exec(p)* means *p* contains the execution permission. *socket(o)* holds when *o* refers to a socket.

APPENDIX C ADDITIONAL EXPERIMENT RESULTS

A. False Alarm Entity Reduction

Notably, in simple scenarios such as S-2 and S-3, the size of the malicious sub-graph is marginally reduced. This is primarily because most malicious activities and related entities in these simulated environments are not seen during the training stage. However, CAPTAIN can still reduce the false alarms by adjusting the alarm threshold.

In addition to minimizing false alarms, we also want to reduce the number of suspicious nodes in the provenance graph, thereby expediting forensic investigations. In forensic analysis using tag-based PIDS, it's essential to examine the subgraph comprising all nodes tagged as malicious to comprehend the attack. Consequently, if malicious tags are widespread throughout the graph, the resulting subgraph may become too large for effective processing and analysis.

TABLE X: Simulated Scenario Summary

Attack Scenario		Attack Description
Malicious	ReverseShell(RS)	Connect to the victim's host, collect system information, and install multiple applications
	WebShell(WS)	Connect to the victim's host, collect system information and modify system configurations
	AttackChain(AC)	A randomly generated attack chain using Atomic Red Team [6]
	Kimsuky(Kim)	A simulated North Korean APT Kimsuky
	Chaos	A malicious payload that allows remote control
Server Environment		App or Process Involved
Benign	Streaming	Kafka, Mysql, Nginx, Redis, Zookeeper
	Developing	Iptables, Zabbix, Gitlab, VSCode, Influxdb, Ixextend, redis-server, Qingtengyun, Baota, docker
	Cloud	finalshell, postgres, web.py, Apache Struts 2, saltstack, Cloud Workload Protection Platforms

TABLE XI: Tag propagation policies

Event	Tag to update	New tag value for different subject types		
			suspect	suspect environment
$create(s, x)$	$x.dtag$	$s.dtag$	$s.dtag$	$s.dtag$
$read(s, x)$	$s.dtag$	$\min(s.dtag, x.dtag)$	$\min(s.dtag, x.dtag)$	$\min(s.dtag, x.dtag)$
$write(s, x)$	$x.dtag$	$\min(s.dtag + a_b, x.dtag)$	$\min(s.dtag, x.dtag)$	$\min(s.dtag + a_e, x.dtag)$
$load(s, x)$	$s.ptag$		$\min(s.ptag, x.itag)$	
	$s.dtag$		$\min(s.dtag, x.dtag)$	
$exec(s, x)$	$s.ptag$	$x.itag$	$\min(x.itag, susp_env)$	$x.itag$
	$s.dtag$	$\langle 1.0, 1.0 \rangle$	$\min(s.dtag, x.dtag)$	$\min(s.dtag, x.dtag)$
$inject(s, s')$	$s'.stag$		$\min(s'.stag, s.itag)$	
	$s'.dtag$		$\min(s.dtag, s'.dtag)$	
$periodically:$	$s.dtag$	$\max(s.dtag, d_b * s.dtag + (1 - d_b) * T_q b)$	no change	$\max(s.dtag, d_e * s.dtag + (1 - d_e) * T_q e)$

TABLE XII: Alarm generation policies

Name	Description	Operation(s)	Data integrity condition	Other conditions
MemExec	Prepare binary code for execution	$mmap(s, p), mprotect(s, p)$	$s.itag < 0.5$	$incl_exec(p)$
FileExec	Execute file-based malware	$exec(s, o), load(s, o)$	$s.itag < 0.5$	$s.ptag > 0.5$
Inject	Process injection	$inject(s, s')$	$s.itag < 0.5$	$s'.ptag > 0.5$
ChPerm	Prepare malware file for execution	$chmod(s, o, p)$	$s.itag < 0.5$	$incl_exec(p)$
Corrupt	Corrupt files	$write(s, o), mv(s, o), rm(s, o)$	$s.itag < 0.5$	-
Escalate	Privilege escalation	$any(s)$	$s.itag < 0.5$	changed userid
DataLeak	Confidential data leak	$write(s, o)$	$s.itag < 0.5$	$s.ctag < 0.5, socket(o)$
MalFileCreation	Ingress Tool Transfer	$create(s, o)$	$s.itag < 0.5$	$File(o)$

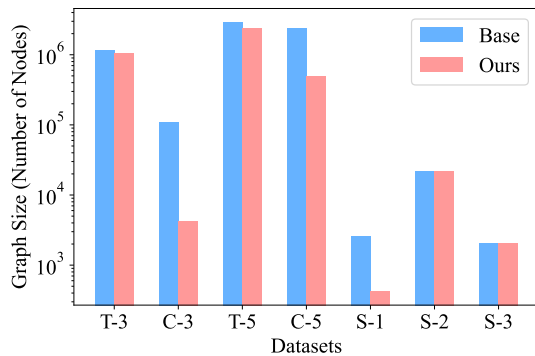


Fig. 7: The comparison between CAPTAIN and the baseline in terms of the numbers of low-integrity nodes in the provenance graph

B. Amount of Gradients to Save During Training

We maintain two dictionaries for each node n to save the gradients of tag_n :

$$\nabla_n^A := \{n' : \frac{\partial tag_n}{\partial a_{n'}}, n' \in N\} \text{ and } \nabla_n^G := \{e : \frac{\partial tag_n}{\partial g_e}, e \in E\}$$

For each node, ∇_A and ∇_G are initialized according to Eq. 8 and Eq. 10. When system events happen on the node, and tags are updated according to the propagation policies, the gradients are also updated. Theoretically, the worst case of memory usage for saving all ∇_n^A is $O(|N|^2)$, and $O(|N||E|)$ for saving all ∇_n^G .

Please note that we only store non-zero gradients in the dictionary. Therefore, although $|N|$ and $|E|$ could be very large in provenance graphs, the size of ∇^A and ∇^G would be reasonable because gradients with the value of zero would not be stored. Every time after the gradients are calculated, we add the non-zero values into ∇_n^A and ∇_n^G and remove the too-small gradients (e.g., $< 10^{-5}$) from the dictionaries. In practice, most gradients would always be zero due to the following three reasons: 1) In most cases, the provenance graph is relatively sparse; a majority of nodes lack connections to other nodes, and only a small fraction of nodes engage in numerous interactions with others. For example, a specific process would only read a small set of files on the system; 2) Even if a node

connects with many different neighbors, the gradients only get updated when the edge (i.e., the corresponding event) changes the tags. Therefore, most benign nodes and edges would not be added to ∇_n^A and ∇_n^G ; 3) As g_e is smaller than 1, some gradients would become near-zero after many iterations, which would be removed from ∇_n^A and ∇_n^G .

We show the distribution of the number of the non-zero gradients that need to be stored during tag propagation in Fig. 8. We use datasets from DARPA Engagements in this experiment because the duration is much longer than others. The histograms clearly illustrate the long-tailed distribution of the non-zero values of gradients for each node, which means we only need to store a tiny number of non-zero gradients for most nodes. The average numbers are less than 5 for all those four datasets. Hence, the additional overhead is reasonable after adding the learning module.

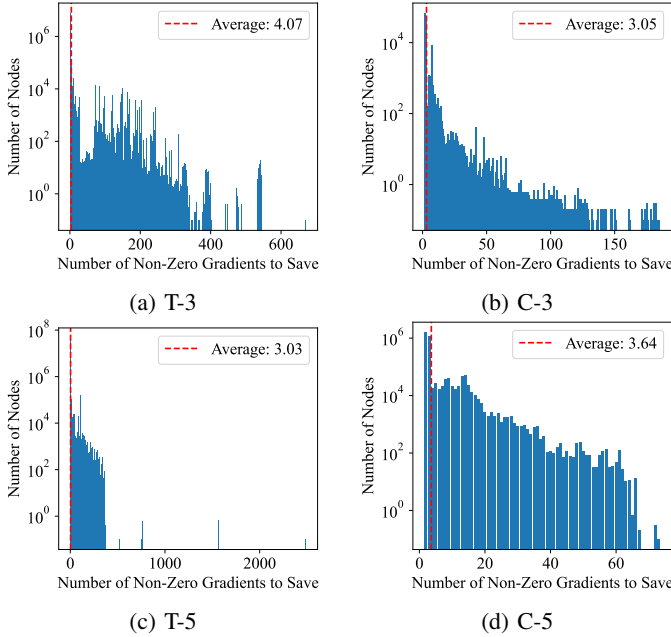


Fig. 8: The distribution of the numbers of non-zero gradients to A and G that each nodes need to save during tag propagation.

C. Mimicry Attack Experiment

Since it's hard to perform mimicry attack behaviors in the DARPA engagement environment, we insert events into the existing DARPA dataset to mimic benign behaviors involving malicious entities. we used the E3 cadets testing set used in FLASH evaluation for this experiment. In the attack, `/tmp/test` file is downloaded and executed, serving as a command and control malware to carry out the rest of the attack. We identified a benign file `/dev/tty` to serve as the target to mimic. Specifically, we replicated interactions with `/dev/tty` on `/tmp/test` to let `/tmp/test` mimic normal behaviors.

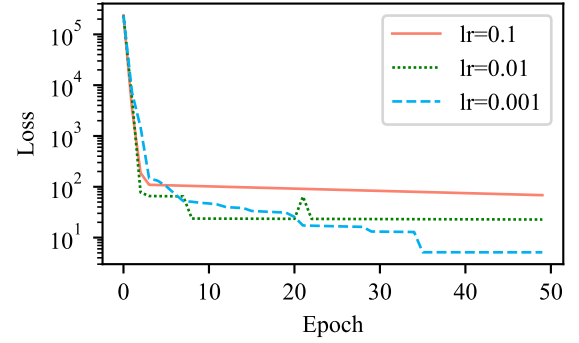


Fig. 9: Training loss using different learning rates (lr).

D. Ablation Study on Learning Rate

Fig. 9 shows the changes of the training loss when we use different learning rates during training. For this experiment, we used CADETS from DARPA Engagement 3. We can see the influence of the learning rates on the training process. In practice, if the training is limited to 20 epochs (due to time and resource issues), a learning rate of 0.01 is advisable; for longer training durations, 0.001 is likely a more preferred choice.